Forensic Science International: Reports 11 (2025) 100418

Contents lists available at ScienceDirect

Forensic Science International: Reports

journal homepage: www.sciencedirect.com/journal/forensic-science-international-reports

Technical note

Technical note: Parameters of bloodstain pattern spatial reconstruction in manual vs. computer-aided data acquisition

Zack Kowalske [a,b,*], David T. Snively [c], Abdulrahman Oleiwi [a,d], Graham Williams [a]

[a] Staffordshire University, School of Health, Education, Policing, and Sciences, College Rd, Stoke-on-Trent ST4 2DE, United Kingdom
[b] Roswell Police Department, Crime Scene Investigations Unit, 39 Hill Street, Roswell, GA 30075, United States
[c] Georgia State University, Department of Criminal Justice and Criminology, 55 Park Place, Atlanta, GA 30303, United States
[d] Centre for Biomedicine, Hull York Medical School, University of Hull, Cottingham Road, Hull HU6 7RX, United Kingdom

ARTICLE INFO

Keywords:
Bloodstain pattern analysis
Angle of impact
Area of origin
FARO zone
Computer aided

ABSTRACT

This study compares the accuracy and precision of manual and computer-aided methods in bloodstain pattern analysis using equine blood under controlled conditions. Manual measurements by experienced analysts were compared to those obtained with FARO Zone 3D (FZ3D). Manual readings of single bloodstains showed higher variability and lower accuracy, while FZ3D improved angle calculations due to enhanced precision. Differences in determining the area of convergence and origin were minimal, but FZ3D offered greater workflow efficiency and data visualization. The findings highlight the need for independent validation of BPA methods and support integrating computer-aided techniques for more accurate, efficient forensic analyses.

Introduction

The spatial reconstruction of bloodstain impact patterns uses the measurements of individual bloodstains to determine three key parameters: the angle of impact, the area of convergence, and the area of origin. These three parameters aid in interpreting from where liquid blood originated in event reconstructions. Bloodstain measurement, data analysis, and spatial pattern visualizations have evolved from human-based manual methods to computer-aided software-based methods. It is critical to make comparisons between the manual and computer-aided methods to validate methods in a process that is independent of the validation provided by the commercial manufacturer of software [1–3]. This independent validation provided an added foundation of use in competency and proficiency applications, as well as identified a normal range of acceptable results. In this study, the accuracy and precision of manual, examiner-based data acquisition were compared to computer-aided data acquisition using the FARO Zone 3D (FZ3D) Expert software. This study was based on laboratory-produced individual bloodstains and impact patterns of known spatial origin using equine blood.

Materials and methods

Blood source

The blood source used for this research was equine whole blood in citrate anticoagulant preservative from HemoStat Laboratories (Dixion, California). Equine blood was selected for this study due to commercial availability, relative consistency, reduced biosafety concerns compared to human blood, and validation for forensic use in previous studies [4,5]. The blood was divided into 5 mL samples in plastic tubes and stored refrigerated, with the bloodstock being utilized in the experiments within fourteen days from the initial blood draw days [6]. Prior to conducting experiments, the necessary volume of blood was removed and subjected to manual agitation to ensure homogeneity. Afterward, the samples were heated to 37° C using a water bath. Experimentation was conducted in the Roswell Police Department's Forensic Science Laboratory Experiment Room at 22° C ambient temperature and no detectable air current.

Single blood drop angle of impact study

White, 50 lb. craft paper, commonly used in BPA training and experimentation, was used as the target surface on which the single

* Corresponding author at: Staffordshire University, School of Health, Education, Policing, and Sciences, College Rd, Stoke-on-Trent ST4 2DE, United Kingdom.
E-mail address: zkowalske@roswellgov.com (Z. Kowalske).

https://doi.org/10.1016/j.fsir.2025.100418
Received 7 February 2025; Received in revised form 9 May 2025; Accepted 11 May 2025
Available online 12 May 2025
2665-9107/

stains were deposited at a known angle of impact. A section of paper, approximately 10 in. x 10 in., was placed on an adjustable surface that could be oriented to a given angle relative to the falling blood flight path. The angles used for this study were 90°, 75°, 60°, 45°, and 30°, which were confirmed with a digital Leica Disto inclinometer. A BrandZig 3 mL syringe with a one inch 23-gauge needle was clamped to a laboratory bench ring stand with the needle open tip measured at one meter above the target (Fig. 1). The agitated and heated bloodstock was drawn into the syringe and ten drops were deposited onto the target paper at the known angle, with the target adjusted between drops to prevent overlap. The needle was wiped between drops to prevent the buildup of any blood which might alter the drop size. The syringe and needle were replaced at each new angle being used.

The resultant bloodstains deposited on the target were allowed to dry for approximately ten minutes and then photographed using a Fuji XT1 DLSR camera with a metric scale in the image following standard BPA documentation practices [7,8]. The digital images were used to manually measure the bloodstain width and length by the author (single examiner study) and ten participating independent examiners (multiple examiner study). The length of the stain, or the major axis, is the longest line segment within an elliptical stain. The width of the stain was defined as the minor axis measurement or the longest line segment perpendicular to the major axis within an elliptical stain. For Circular stains, the width and length are measurements perpendicular to one another that have the same value. The independent examiners consisted of ten bloodstain pattern analysts who volunteered in response to a solicitation placed on a professional networking website. They ranged from 1 to 20 years in BPA experience and hailed from the United States, the Philippines, Italy, and Argentina. Each examiner was provided the digital images with scale and instructed to manually measure each stain, using the manual measurement method of their choice, and recording their measurements on a provided measurement log. Each of the ten volunteer analysts measured the angle of impact once per stain. The images were not re-randomized for repeat measurements, limiting the study to a singular measurement observation of ten unknown stains. They were not provided with any information on the purpose of the study.

The compiled bloodstain width and length data was used by the author to calculate the stain angle of impact, using the Eq. 1, the commonly documented BPA geometric formula [9,10]. The mathematical mean and standard deviation for each angle of impact were calculated, with the standard deviation being the measured range of variation from the calculated mean of a sample set.

$$\theta = \sin^{-1}\left(\frac{width}{length}\right) \quad (1)$$

also expressed as angle of impact = arcsine (width/length)

Bloodstain100418 impact pattern area of convergence and origin study

A three-walled room measuring 2 m x 2 m x 2 m was constructed within the laboratory using construction timber and panel walls. The floor and walls were lined with white target paper. An impact pattern-generating mechanism consisting of a 3.2 cm wide wooden dowel operated by tension bands (following the design described by Attinger et al. [11]) was placed in the middle of the experimental room (Fig. 2).

The impact pattern was created by a wooden dowel rotating under the tension of rubber bungee cords, striking liquid blood on a hockey puck. The apparatus was placed in a manner that the hockey puck surface was one meter from the center of each wall and one meter above the floor. An adjustable single channel pipettor was used to deposit 5 mL of agitated and heated blood onto the puck's upper surface. The dowel rod was set and held in the ready position with a safety chuck. The chuck was pulled by an affixed rope which caused the dowel rod to be drawn down by the tension bands and strike the liquid blood, producing an impact pattern. This process was repeated to obtain 10 separate impact patterns.

The stains and patterns were photographed following standard BPA documentation practices [7,8]. Still images were captured with a Fuji XT1-UV/IR mirrorless camera. The images were captures at the highest resolution using three lens variants based on the stain imaging requirement: a Fujinon Aspherical Super EBC f= 60 mm 1:2.4 lens, a Fujinon Aspherical Super EBC XF 18–135 mm 1:3.5–5.6 R LM OIS W*R* lens, and a Fujinon Aspherical Nano-GI XF 16 mm 1:1.4 R W*R* lens. The ISO, f-stop, and shutter speed were adjusted to capture clear images for analysis. The sections of target paper with each stain pattern were used for manual stain measurements and area of convergence/origin determination. The digital images of each stain pattern was used in the computer aided parameter determinations using the FZ3D software according to manufacturer's instructions and applications.

The manual method of impact pattern reconstruction used a trigonometric method [14]. This method required the selection of 15–20 stains from within each pattern. Stain selection required discernable

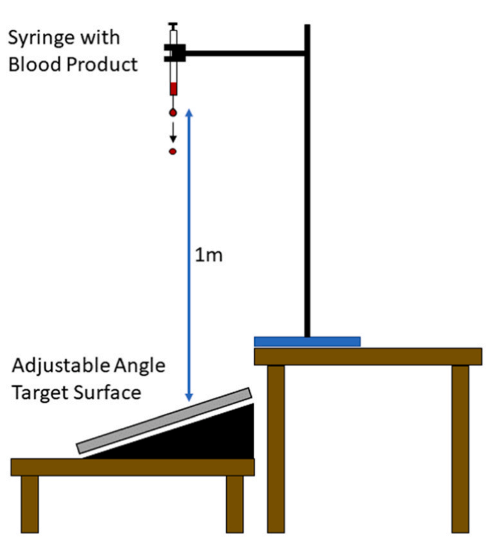

Fig. 1. Single drop angle of impact setup diagram.

Fig. 2. Tension Based Impact Spatter Pattern Mechanism.

directionality and a defined inception point boarder. The manual stain measurements were collected using a loupe with 1/10 mm base scale increments. Each stain was measured, and the angle of impact was calculated. A line was drawn through the long axis of each selected stain in the opposite direction of its flight path graphically revealing the general intersection of flight paths, which is referred to as the area of convergence (AOC).

A box was drawn with the line of each side affixed to the furthest intersecting flight path. The mathematical average center of the box was defined as the Area of Convergence Mean. The distance from each selected stain's leading edge to the Area of Convergence Mean was used in Eq. 2 to determine the distance from the target to the calculated point of origin (Φ). Eqs. 1 and 2 represent the standard trigonometric relationships used in angle-of-impact and area-of-origin calculations in BPA [9,10]. They are presented here to illustrate the analytical steps used in this study. The 15–20 points of origin for a given pattern were then used to provide the estimated area of origin (AOO). This was determined for all ten impact patterns.

$$\Phi = \tan(\text{angle of impact})(\text{distance to mean area of convergence}) \quad (2)$$

The computer-aided bloodstain impact pattern reconstruction was accomplished with images imported into the FZ3D Blood Spatter Analysis module. Each image was scaled and aligned, and 15–20 stains were selected using the ellipse measuring tool. The selected stains did not necessarily correspond with those chosen during the manual AOC/AOO process. Although this could be considered a methodological limitation, the analysis did not reveal any statistically significant differences in the AOC/AOO results that would meaningfully affect the study's conclusions. FZ3D uses these selections to automatically calculate the area of origin and provide a graphic X, Y, and Z coordinate view with standard deviation data (Fig. 3).

Results

Figs. 4 and 5 summarize the mean, range and standard deviations found when manually determining the angle of impact for ten single blood stains dropped on a target at each of the known (based on setup) angles of impact of 30°, 45°, 60°, 75°, and 90°.

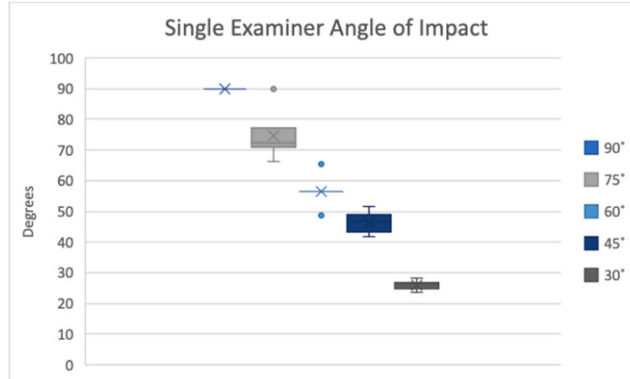

Fig. 4. Single examiner determinations of the angle of impact showing the mean (x), range (line bar) and standard deviation (color bar) at five known angles for 10 stains at each known angle.

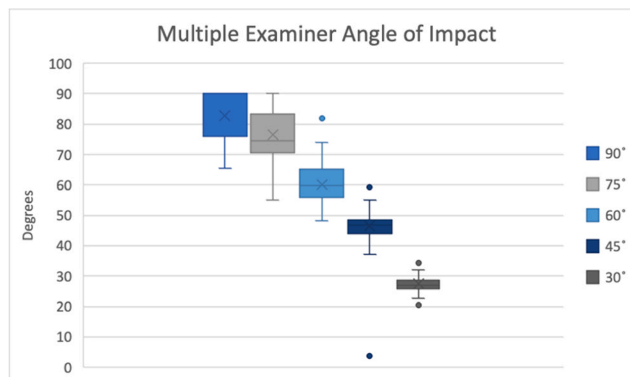

Fig. 5. Multiple examiners (10) determinations of the angle of impact showing the mean (x), range (line bar), and standard deviation (color bar) at five known angles for 10 stains at each known angle.

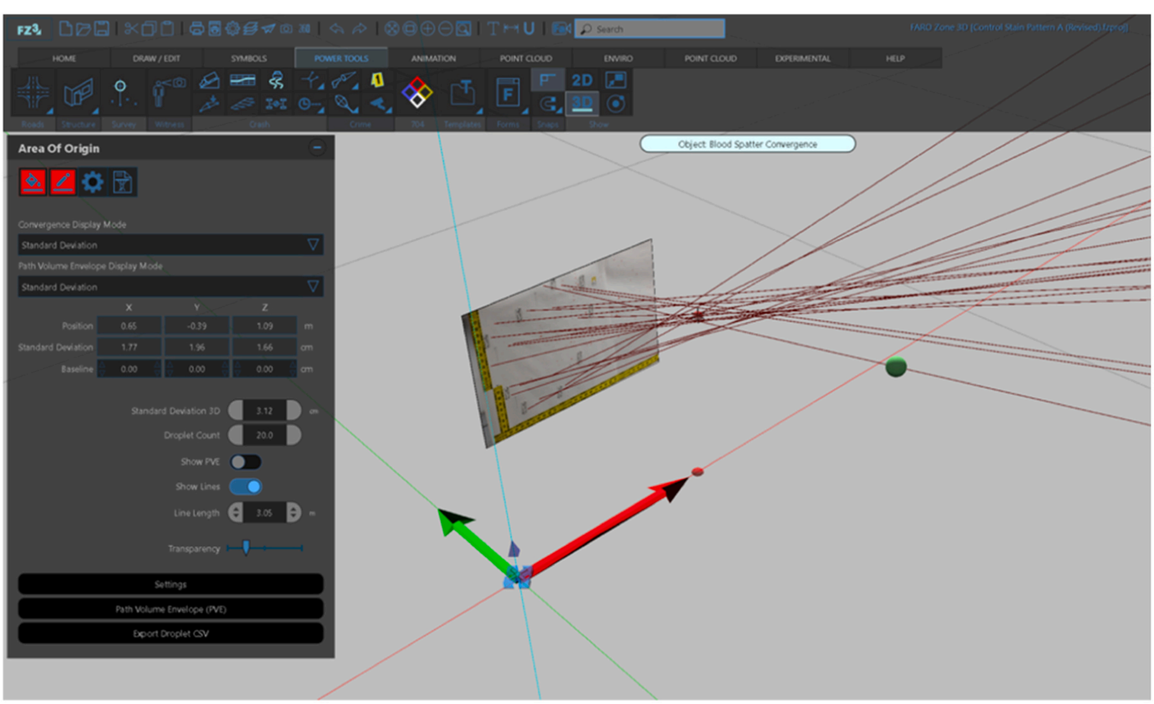

Fig. 3. Example of FZ3D calculated area of origin and X, Y, and Z position representation.

Fig. 6 summarizes the calculated area of origin X, Y, and Z coordinates for ten impact patterns analyzed by computer-assisted measurements (ellipse tool). Table 1 summarizes the results of the manual versus the FZ3D computer-assisted area of origin determinations, showing the X, Y, and Z coordinates of the ten impact patterns produced and used in this study. The known setup coordinates were an X, Y and Z at 1 m each.

Discussion

The material substitution of human blood within bloodstain pattern analysis (BPA) research has been extensively studied. Using certain synthetic fluids and animal species' blood are acceptable replacements [5,6,12,13]. Previous literature concluded that the use of an anticoagulant has negligible impact on the bloodstains and patterns produced by the blood product, and suggested the preserved blood can be used for up to fourteen days [4–6]. Using equine blood, as opposed to human blood, offered commercially available and consistent sourcing, eliminated the risk from human blood borne pathogens, and mitigated ethical concerns. The use of equine blood throughout this study should not have had any substantial influence on the results obtained for comparison purposes. It is acknowledged that the results presented in this study were obtained under controlled laboratory conditions, which are rarely replicated in real-world crime scene environments. However, these conditions were intentionally selected to ensure a valid baseline comparison between human analysis and computer-aided results. The findings serve as a foundational reference point and inherently suggest the need for further validation in more complex and realistic scenarios, such as those involving varied surface roughness, porosity, and other environmental factors.

Angle of Impact. Review of the data generated from the manual determination of the angle of impact shows an apparent correlation between the angle of impact and the accuracy of the examiner's measurements. As the angle approaches the orthogonal (90̊) to the target surface, the accuracy and precision of the examiner's measurements is diminished as the angle approaches the orthogonal (90̊). This is seen as an increasing measure of standard deviation among the respective angles of impact (Table 2). This trend is previously studied and suggests that the angles closer to 90̊ have more visual ambiguity leading to the examiner's inability to accurately measure the stains [13,14]The standard deviations were generally greater for the collective data of the 10 examiners than for the single examiner data. This is, at least in part, a reflection of inter-examiner variability contributing to the standard deviation, which is not a contributing factor in the single examiner situation. This is one reason that primarily only single examiner data was compared against that of FZ3D. Though this approach could introduce some author bias, the single-examiner measurements serve as a reference baseline; results from multiple independent examiners are presented separately to illustrate broader variability.

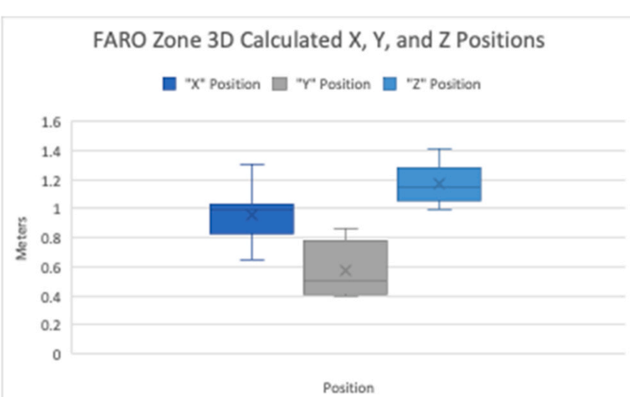

Fig. 6. Computer-assisted Area of Origin coordinates for 10 impact patterns known to be made at 1 m x 1 m x1m.

Table 1
Comparison of Manual and FZ3D AO Estimation Coordinates.

Examiner-Based AO Estimation			
	X- Coordinate (Meters)	Y-Coordinate (Meters)	Z-Coordinate (Meters)
Calculated Mean	1.04	0.77	1.11
Difference from Actual	0.04	0.23	0.11
Standard Deviation	0.17	0.17	0.18
FZ3D-Based AO Estimation			
	X- Coordinate (Meters)	Y-Coordinate (Meters)	Z-Coordinate (Meters)
Calculated Mean	0.98	0.59	1.18
Difference from Actual	0.02	0.41	0.18
Standard Deviation	0.15	0.18	0.14

Table 2
Comparison of Manual and FZ3D angle of impact calculated mean and standard deviation.

	Manual AOI Analysis (Author)				
True Angle of Impact	90	75	60	45	30
Calculated Mean	90	74.7	56.5	46.2	26
Standard Deviation	0	8.3	3.9	3.4	1.4
	FZ3D-Aided AOI Analysis (Author)				
True Angle of Impact	90	75	60	45	30
Calculated Mean	90	67.5	54.4	41.2	25.6
Standard Deviation	0	3.8	2.2	2.3	2.3
	Manual AOI Analysis (Multiple Examiner Trial)				
True Angle of Impact	90	75	60	45	30
Calculated Mean	85	71.7	59.6	49.2	26.6
Standard Deviation	10.3	13	6.3	5	3

When the single examiner manual data is compared to that of the FZ3D aided data, both of which were conducted by the author, we see improved accuracy in both the calculated mean and standard deviation. This is attributed to the precision of measurement provided by the FZ3D ellipse measuring tool and the discernibility of stain edge provided by digitally aided resolution.

Area of Convergence. When comparing the manual versus the FZ3D-aided results of the X,Y, and Z coordinates, the X and Z represent the proximity to the AOC mean. The data describes little variation between the methods, being within 6 cm of each other on both planes and a difference of 1 cm in standard deviation. This demonstrates the reliability of the "box method" in AOC estimation methodology. While it is recognized that multiple analysts could strengthen the repeatability result of this AOC methodology, the AOC and AOO portions were performed by a single examiner to provide a direct comparison to the FZ3D workflow under easily manageable, uniform conditions.

Area of Origin. Within the data, the Y-Coordinate in Table 1 represents the distance from the target to the AOO. FZ3D and manual methodologies yielded closely matched results in determining the AOO. The methods were within 18 cm of each other's mean and within 1 cm of calculated standard deviation. Thus, as it relates to the area of origin estimation, there is little difference in accuracy between the manual and the computer-aided methodologies. The principal advantage of computer-aided methods lies in their efficiency, comprehensive statistical analysis, and minimization of human error.

Conclusion

Three-dimensional reconstruction methodologies for bloodstain patterns have undergone transformative technological advancements. BPA event reconstruction has progressed from rudimentary techniques such as "pulling string" to 21st-century computer-aided software applications. In contemporary forensic applications, examiners should be more inclined to leverage the reliability of trigonometric mathematical calculations or the precision of specialized software like FARO Zone 3D. This study validates the reliability of computer-assisted data acquisition, comparing manual and computer-assisted measurements, and providing useful insights into assessing competency in these techniques. This has demonstrated that the methods used are applicable for future research, establishing a known baseline of AOI/AOC/AOO variation. This allows for a better assessment of variability in experimental results in the follow-on substrate influences studies. Although this study demonstrates a preliminary comparison of manual and computer-aided methods, a comprehensive, randomized experimental design with repeated measures is recommended for an in-depth evaluation of variability and bias.

CRediT authorship contribution statement

Kowalske Zack: Writing – review & editing, Writing – original draft, Visualization, Validation, Software, Resources, Project administration, Methodology, Investigation, Funding acquisition, Formal analysis, Data curation, Conceptualization. **Oleiwi Abdulrahman:** Writing – review & editing, Supervision. **Snively David:** Visualization, Formal analysis. **Williams Graham:** Writing – review & editing, Supervision, Methodology.

Sources of funding

Dan Rahn Research Grant, funded by the International Association of Bloodstain Pattern Analysts

Declaration of Generative AI and AI-assisted technologies in the writing process

During the preparation of this work, the author(s) used ChatGPT4 (OpenAI, San Francisco, California) and Grammarly (Grammarly, San Francisco, California) in order to improve readability and language syntax of the initial authored draft. After using this tool/service, the author(s) reviewed and edited the content as needed and take(s) full responsibility for the content of the publication.

Declaration of Competing Interest

None

Acknowledgments

Lynne D. Herold, PhD. for her guidance and consultation on experimental design.

References

[1] L. Carter,A, J. Forsythe-Erman, M. Illes, P. Laturnus, G. Lefebvre, C. Stewart, et al., Validation of the backtrack suite of programs for bloodstain pattern analysis, J. Forensic Identif. 56 (2) (2006) 242–254.
[2] K. Maloney, J. Kileen, A. Maloney, Use of hemospat to include bloodstains located on nonorthogonal surfaces in area-of origin calculations, J. Forensic Identif. 59 (5) (2009) 513–524.
[3] E. Liscio, A preliminary validation for the FARO zone 3D area of origin tool, J. Assoc. Crime. Scene Reconstr. (2018).
[4] Brownson,D.A.C.;Banks C.E.;El-Sayed M.;Brownson D.A.C., Banks C.E. *Crime Scene Investigation II: The Effect of Warfarin on Bloodstain Pattern Analysis Detection of Caffeine at various Temperatures using MIP's View Project Materials Chemistry View Project Crime Scene Investigation II: The Effect of Warfarin on Bloodstain Pattern Analysis*. -07 2015.
[5] Miles,H. Bloodstain Pattern Analysis: Developing Quantitative Methods of Crime Scene Reconstruction through the Interpretation and Analysis of Environmentally Altered Bloodstains. Level of Thesis, University College London, 2014.
[6] M. Raymond, E.R. Smith, J. Liesegang, The physical properties of blood - forensic considerations, Sci. Justice 36 (3) (1996) 153–160.
[7] T. Bevel, R.M. Gardner. Bloodstain Pattern Analysis With An Introduction to Crime Scene Reconstruction, 3rd ed., CRC Press, Boca Raton, FL, 2008.
[8] R. Gardner, D. Krouskup. Practical Crime Scene Processing and Investigation, 3rd ed., CRC Press, Boca Raton, FL, 2018.
[9] C. Rizer, Police mathematics; a textbook in applied mathematics for police, Charles C Thomas, Springfield, IL, United States, 1955.
[10] H. MacDonnell, Flight Characteristics and Stain Patterns of Human Blood, National Institute of Law Enforcement and Criminal Justice, Washington D.C., 1971.
[11] D. Attinger, Y. Liu, T. Bybee, K. De Brabanter, A data set of bloodstain patterns for teaching and research in bloodstain pattern analysis: impact beating spatters, Data Brief. 18 (2018) 648–654.
[12] D.V. Christman, A Study Comp. Contrast Anim. Blood Hum. Blood Prod. (1997).
[13] Spivey,D.G. Effect of Wind on Region of Origin Calculations of Impact Bloodstain Patterns: Implications for Bloodstain Pattern Analysis. Level of Thesis, University of Western Australia, 2016.
[14] Dynamics of Blood Drop Formation and Flight. Available Online: https://search.datacite.org/works/10.26021/2745.